Combining the Hybrid Mimetic Mixed method and the Eulerian Lagrangian Localised Adjoint Method for approximating miscible flows in porous media.

Hanz Martin Cheng and Jérôme Droniou

Abstract We design a numerical scheme for a miscible displacement in porous media. This scheme is based on the Hybrid Mimetic Mixed method, which is applicable on generic meshess, and uses a characteristic method for dealing with the advection.

1 Introduction

One of the tertiary oil recovery processes consists in injecting, in an underground oil reservoir, a solvent that mixes with the residing oil and reduces its viscosity, thus enabling its displacement towards a production well. Let Ω be a bounded domain in $\mathbb{R}^d$ and $[0,T]$ be a time interval. Denote by $\mathbf{K}(\mathbf{x})$ and $\varphi(\mathbf{x})$ the permeability tensor and the porosity of the medium, respectively. Neglecting gravity, the mathematical model is [8]:

$$\nabla \cdot \mathbf{u} = q^+ - q^- := q \qquad \text{on } \Omega \times [0,T]$$
$$\mathbf{u} = -\frac{\mathbf{K}}{\mu(c)}\nabla p \qquad \text{on } \Omega \times [0,T] \tag{1a}$$

$$\varphi\frac{\partial c}{\partial t} + \nabla \cdot (\mathbf{u}c - \mathbf{D}(\mathbf{x},\mathbf{u})\nabla c) = q^+ - cq^- := q_c \qquad \text{on } \Omega \times [0,T] \tag{1b}$$

This coupled system of PDEs has unknowns $p(\mathbf{x},t)$ the pressure of the mixture, $\mathbf{u}(\mathbf{x},t)$ the Darcy velocity, and $c(\mathbf{x},t)$ the concentration of the injected solvent. The functions q^+ and q^- represent the injection and production wells respectively, and $\mathbf{D}(\mathbf{x},\mathbf{u})$ denotes the diffusion tensor

$$\mathbf{D}(\mathbf{x},\mathbf{u}) = \varphi(\mathbf{x})\left[d_m\mathbf{I} + d_l|\mathbf{u}|\mathscr{P}(\mathbf{u}) + d_t|\mathbf{u}|\left(\mathbf{I} - \mathscr{P}(\mathbf{u})\right)\right] \text{ with } \mathscr{P}(\mathbf{u}) = \left(\frac{u_i u_j}{|\mathbf{u}|^2}\right)_{i,j}.$$

School of Mathematical Sciences, Monash University, Victoria 3800, Australia, e-mail: hanz.cheng@monash.edu, jerome.droniou@monash.edu

Here, d_m is the molecular diffusion coefficient, d_l and d_t are the longitudinal and transverse dispersion coefficients respectively, and $\mathscr{P}(\mathbf{u})$ is the projection matrix along the direction of $\mathbf{u}$. Also, $\mu(c) = \mu(0)[(1-c) + M^{1/4}c]^{-4}$ is the viscosity of the fluid mixture, where $M = \mu(0)/\mu(1)$ is the mobility ratio of the two fluids. We consider no-flow boundary conditions and, as usual for this process, zero initial conditions for the concentration:

$$\mathbf{u} \cdot \mathbf{n} = (\mathbf{D}\nabla c) \cdot \mathbf{n} = 0 \text{ on } \partial\Omega \times [0,T], \qquad c(\cdot,0) = 0 \text{ in } \Omega. \tag{1c}$$

The pressure is fixed by imposing a zero average: for all $t \in [0,T]$, $\int_\Omega p(\mathbf{x},t)\mathrm{d}\mathbf{x} = 0$

A number of numerical schemes have been considered for this model, some of which are the Mixed Finite Element–Eulerian Lagrangian Localised Adjoint Methods (MFEM–ELLAM) [10] and a Mixed Finite Volume (MFV) scheme with up-winding [3]. Due to the use of finite element methods, the MFEM–ELLAM is only limited to certain types of meshes. Moreover, a large number of quadrature points is required to produce acceptable results [9]. The MFV (part of the Hybrid Mimetic Mixed (HMM) schemes, which contain in particular mixed-hybrid Mimetic Finite Differences [5]) is adapted to more generic meshes, but the upwinding tends to introduce excess diffusion in the solution. The purpose of this paper is to discretise (1) using the HMM method, thus allowing for generic meshes, and using the ELLAM for the advective term, to avoid the pitfalls of upwinding.

2 The HMM–ELLAM

We consider polytopal meshes as defined in [4], in dimension $d = 2$. Thus, $\mathscr{T} = (\mathscr{M}, \mathscr{E}, \mathscr{P})$ are the set of cells, edges, and points of our mesh, respectively. $\mathscr{E}_K \subset \mathscr{E}$ denotes the set of edges of the cell $K \in \mathscr{M}$. A usual way to approximate (1) is to use a two-step process. Starting from a known value $c^{(n)}$ of c at time level n (for $n = 0$, $c^{(0)} = 0$), a numerical solution $p^{(n+1)}$ for p at time level $n+1$ is computed by approximating (1a) with $c = c^{(n)}$. This computation also provides an approximation $\mathbf{u}^{(n+1)}$ of the Darcy velocity at time level $n+1$, and possibly of secondary quantities (e.g., fluxes). The concentration $c^{(n+1)}$ at time level $n+1$ is then computed by approximating (1b) by using $\mathbf{u} = \mathbf{u}^{(n+1)}$ and the aforementioned secondary quantities.

2.1 Numerical Scheme for the Pressure Equation

Incorporating $\int_\Omega p = 0$, the variational formulation for (1a) for each cell $K \in \mathscr{M}$ is then given by

$$\int_K \frac{\mathbf{K}}{\mu}\nabla p \cdot \nabla v - \int_{\partial K} \frac{\mathbf{K}}{\mu}\nabla p \cdot \boldsymbol{n}_{K,\sigma} v + \int_\Omega p \int_K v = \int_K qv, \quad \forall v \in H^1(\Omega). \tag{2}$$

We present the HMM method in its "finite volume" form, see e.g. [5]. The space of degrees of freedom is $X_{\mathscr{T}} := \{w = ((w_K)_{K \in \mathscr{M}}, (w_\sigma)_{\sigma \in \mathscr{E}_K})\}$. For $\sigma \in \mathscr{E}_K$, denote by $T_{K,\sigma}$ the triangle with vertex $\mathbf{x}_K$ and base σ (see Fig. 1), and define

$$\forall w \in X_{\mathscr{T},0}, \ \nabla_H w(\mathbf{x}) = \overline{\nabla}_K w + \frac{\sqrt{2}}{d_{K,\sigma}}[w_\sigma - w_K - \overline{\nabla}_K w \cdot (\overline{\mathbf{x}}_\sigma - \mathbf{x}_K)]\mathbf{n}_{K,\sigma}, \quad (3)$$

where $\overline{\nabla}_K w = |K|^{-1} \sum_{\sigma \in \mathscr{E}_K} |\sigma| w_\sigma \mathbf{n}_{K,\tilde{\sigma}}$ is a linearly exact discretization of the gradient (it is exact if $(w_\sigma)_{\sigma \in \mathscr{E}_K}$ interpolate an affine function at the edge midpoints) and $d_{K,\sigma}$ is the orthogonal distance between $\mathbf{x}_K$ and σ.

The concentration at time n is also approximated in $X_{\mathscr{T}}$, and so cell values $(c_K^n)_{K \in \mathscr{M}}$ are accessible. We use them to define the pressure fluxes by:

$$\forall K \in \mathscr{M}, \ \forall v \in X_{\mathscr{T}}, \ \sum_{\sigma \in \mathscr{E}_K} F_{K,\sigma}(v_K - v_\sigma) = \int_K \frac{\mathbf{K}(x)}{\mu(c_K^n)} \nabla_H p(\mathbf{x}) \cdot \nabla_H v(\mathbf{x}) d\mathbf{x}.$$

The discrete form of (2) then follows easily. Taking test functions so that $v_K = 1$ for cell K and 0 for all other cells gives the balance of fluxes, whilst choosing $v_\sigma = 1$ for an edge σ gives either the flux conservativity (internal edges) or the no-flow boundary conditions (boundary edges). The final scheme for the pressure, which provides $p^{(n+1)} \in X_{\mathscr{T}}$, as well as fluxes $(F_{K,\sigma})_{K \in \mathscr{M}, \sigma \in \mathscr{E}_K}$, is therefore

$$\sum_{\sigma \in \mathscr{E}_K} F_{K,\sigma} + |K| \sum_{M \in \mathscr{M}} |M| p_M = \int_K q. \quad (4)$$

$$\begin{aligned} F_{K,\sigma} + F_{L,\sigma} = 0 \quad &\text{for all edge } \sigma \text{ between two different cells } K \text{ and } L, \\ F_{K,\sigma} = 0 \quad &\text{for all edge } \sigma \text{ of } K \text{ lying on } \partial\Omega. \end{aligned} \quad (5)$$

2.2 Reconstruction of a Darcy velocity

The ELLAM requires to compute the characteristics of the advective component of (1b), that is the solution, for each $\mathbf{x} \in \Omega$, to the ODEs

$$\frac{d\hat{\mathbf{x}}}{dt}(t) = \frac{\mathbf{u}^{(n+1)}(\hat{\mathbf{x}}(t),t)}{\varphi(\hat{\mathbf{x}}(t))}, \qquad \hat{\mathbf{x}}(t^{(n+1)}) = \mathbf{x}. \quad (6)$$

This obviously requires to reconstruct a Darcy velocity $\mathbf{u}^{(n+1)}$ everywhere. Two important features of this velocity need to be accounted for: the no-flow boundary conditions $\mathbf{u}^{(n+1)} \cdot \mathbf{n} = 0$ on $\partial\Omega$, which ensures that the solutions to (6) do not exit the computational domain, and the preservation of the divergence in (1a), to avoid creating regions with artificial wells or sinks (which lead to non-physical flows).

Preserving these features is done by using the technique of [7]. Each cell $K \in \mathscr{M}$ is split into triangles (see Fig. 1), and an oriented interior flux F_{σ^*} is computed on

each internal edge created by this subdivision. Then, $\mathbf{u}^{(n+1)}$ is the $\mathbb{R}\mathbb{T}_0$ function reconstructed from these fluxes on the triangular subdivision. This function belongs to $H_{\mathrm{div}}(\Omega)$ and, to ensure that its divergence is as dictated by (1a), the internal fluxes F_{σ^*} are constructed so that their balance (along with the fluxes $F_{K,\sigma}$ at the boundary of K) in each triangle corresponds to the balance over the cell K:

$$\forall \sigma \in \mathscr{E}_K, \quad \frac{1}{|T_{K,\sigma}|}\left(\sum_{\sigma^* \in \mathscr{E}_{K,\sigma}^{*,\mathrm{int}}} s_{\sigma^*}^{\sigma} F_{\sigma^*} + F_{K,\sigma}\right) = \frac{1}{|K|}\sum_{\sigma' \in \mathscr{E}_K} F_{K,\sigma'},$$

where $s_{\sigma^*}^{\sigma} = 1$ if F_{σ^*} is oriented outside $T_{K,\sigma}$ and -1 otherwise. This local system of equations is underdetermined. The chosen solution is that of minimal l^2 norm.

Fig. 1: Triangulation of a generic cell. Here, $s_{\sigma^*}^{\sigma} = +1$ and $s_{\sigma^{**}}^{\sigma} = -1$.
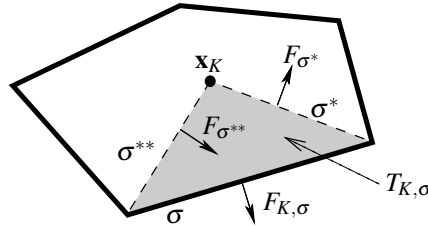
2.3 Numerical Scheme for the Concentration Equation

As with the pressure equation, we multiply the concentration equation (1b) by a test function v and perform integration by parts to obtain

$$\int_{t^n}^{t^{n+1}} \int_{\Omega} \left(\varphi \frac{\partial(cv)}{\partial t} + D\nabla c \cdot \nabla v\right) - \int_{t^n}^{t^{n+1}} \int_{\Omega} c(\varphi v_t + u \cdot \nabla v) = \int_{t^n}^{t^{n+1}} \int_{\Omega} q_c v. \quad (7)$$

The test functions are then selected to eliminate the advective term, and to match the piecewise constant functions at the core of the HMM method. We therefore take v such that $\varphi v_t + \mathbf{u}^{n+1} \cdot \nabla v = 0$ in the sense of distributions, and $v(t^{(n+1)}, \cdot) = \mathbf{1}_K = 1$ on K and 0 outside K. With characteristics computed through (6), this leads to $v(t^{(n)}, \mathbf{x}) = \mathbf{1}_K(\hat{\mathbf{x}}) = \mathbf{1}_{\hat{K}}(\mathbf{x})$, where $\hat{K}$ is K traced back from $t^{(n+1)}$ to $t^{(n)}$ through (6).

The diffusion term is discretised separately from the advective term, by using an implicit scheme. Fluxes $D_{K,\sigma}$ are defined as for the pressure equation (1a), using a piecewise Darcy velocity $\mathbf{u}^{(n+1)}$ given by the reconstructed pressure gradient (3) and the viscosity at $c^{(n)}$. For the source term, we also treat c implicitly. Without

discretising the source term, this leads to the following scheme for (7):

$$\varphi \int_K c^{n+1} - \varphi \int_{\hat{K}} c^n + \Delta t \sum_{\sigma \in \mathscr{E}_K} D_{K,\sigma} = \int_{t^n}^{t^{n+1}} \int_\Omega q_{c^{n+1}} v.$$

For each cell K, the traceback region $\hat{K}$ is approximated in the following manner: for each of the vertices and edge midpoints of K, we solve (6) starting from $\mathbf{x} =$ that vertex or midpoint, we then compute $\hat{\mathbf{x}}(t^{(n)})$ and we approximate $\hat{K}$ by the polygon defined by these points $\hat{\mathbf{x}}(t^{(n)})$. The integrals are then computed by writing $\varphi \int_K c^{n+1} = \varphi |K| c_K^{n+1}$ and $\int_{\hat{K}} c^n = \sum_{M \in \mathscr{M}} |\hat{K} \cap M| c_M^n$, which leads to the following discretised form of the concentration equation

$$\varphi |K| c_K^{n+1} + \Delta t \sum_{\sigma \in \mathscr{E}_K} D_{K,\sigma} = \varphi \sum_{M \in \mathscr{M}} |\hat{K} \cap M| c_M^n + \int_{t^n}^{t^{n+1}} \int q_{c^{n+1}}.$$

2.4 The Integral of the Source Term $q_{c^{n+1}}$

For the integral involving the source term, we use a weighted trapezoid rule in time $\int_{t^n}^{t^{n+1}} \int q_{c^{n+1}} = w \int_{\hat{K}} q_{c^{n+1}} + (1-w) \int_K q_{c^{n+1}}$. The left and right rules correspond to $w = 1$ and $w = 0$, respectively. Let E be an injection cell. A proper weight that will yield mass conservation has been derived for Cartesian meshes on [1]. The weight $w = (1 - e^{-\alpha})^{-1} - \alpha^{-1}$, where $\alpha = \Delta t \int_E q^{n+1} / \int_E \varphi$, can easily be generalized for arbitrary meshes. A separate treatment will be made for cells that trace back into the injection well. These integrals will be computed using a forward tracing algorithm as described in [2].

3 Numerical results

We take: $\Omega = (0, 1000) \times (0, 1000)$ ft^2; timestep of $\Delta t = 36$ days; injection well at $(1000, 1000)$ and production well at $(0,0)$, both with flow rate of 30ft^2/day; constant porosity φ=0.1; constant permeability tensor $\mathbf{K} = 80\mathbf{I}$; oil viscosity $\mu(0) = 1.0$ cp; mobility ratio $M = 41$; $\varphi d_m = 0.0$ft^2/day, $\varphi d_l = 5.0$ft, and $\varphi d_t = 0.5$ft.

Figures 2 and 3 show the numerical solution for the concentration at $t = 3$ years on a Cartesian mesh using the left and the right rule, respectively. As can be seen here, the left rule provides us with an underestimate of the concentration at the injection well, and an overestimate somewhere along the neighborhood of the injection well. The right rule, implemented in [10], is also a bad choice since it provides us with an overshoot of the concentration at the injection well, as already proved for the MFEM-ELLAM in [9]. This is due to the fact that all of the source has been dumped into the injection well in one time step.
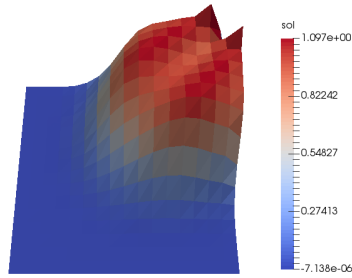
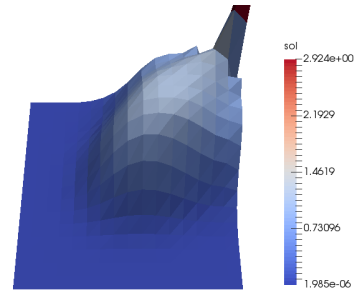Fig. 2: Cartesian mesh, $t = 3$ years, left rule for source terms.

Fig. 3: Cartesian mesh, $t = 3$ years, right rule for source terms.

Figures 4 and 5 show the numerical solution for the concentration using the proper weight for the trapezoidal rule, as described in the previous section. These results present a significant improvement from those obtained through the right and left rule. Numerical results using Hexahedral meshes are presented in Figures 6 and
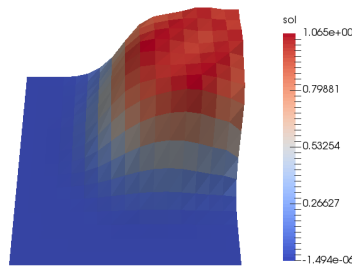

Fig. 4: Cartesian mesh, $t = 3$ years, weighted trapezoid rule for source terms.
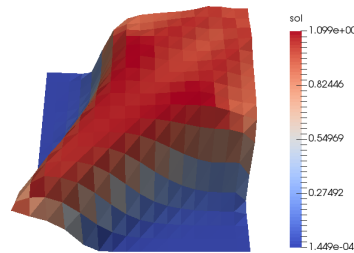
Fig. 5: Cartesian mesh, $t = 10$ years, weighted trapezoid rule for source terms.

7. The concentration spikes up along the boundary at $t = 10$ years. To mitigate this, the approximation of the traceback region is improved by using 3 points per edge (instead of only the edge midpoints); Figures 8 and 9 show the significant improvement this enables. To understand more generally how many points to choose to obtain acceptable approximate traceback regions, we introduce the regularity parameter $m_{\text{reg}} = \max_{K \in \mathcal{M}} (\text{diam}(K)^2/|K|)$ of the mesh. It is then observed a reasonable numerical solution (overshoot $\leq 10\%$) is obtained by taking $\lceil \log_2(m_{\text{reg}}) \rceil$ points along each edge, see Table 1. Further increasing the number of points per edge does not provide any significant improvement to our numerical solution. Finally, we show the numerical solutions for "Kershaw" meshes [6] on figures 10 and 11. We used here a proper quadrature rule for the source term, and an appropriate number of points per edge (see Table 1). The solutions on both Cartesian and hexahedral meshes are very similar, showing a certain robustness of the method with respect to
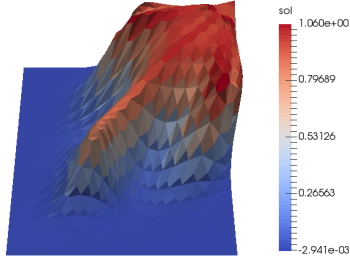
Fig. 6: Hexahedral mesh, $t = 3$ years, weighted trapezoid rule for source terms.
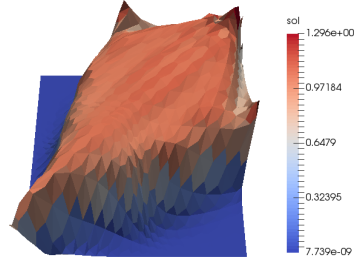

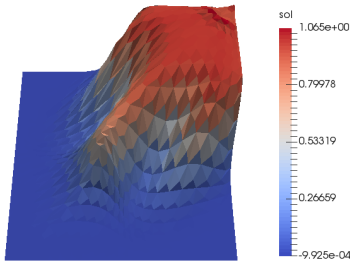Fig. 7: Hexahedral mesh, $t = 10$ years, weighted trapezoid rule for source terms.

Fig. 8: Hexahedral mesh, $t = 3$ years, 3 points per edge, weighted trapezoid rule for source terms.
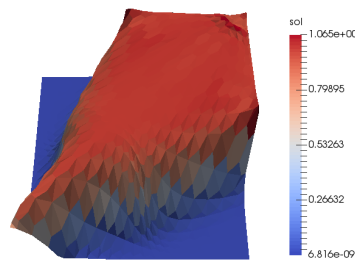

Fig. 9: Hexahedral mesh, $t = 10$ years, 3 points per edge, weighted trapezoid rule for source terms.

Mesh	m_{reg}	$\log_2(m_{\text{reg}})$	points per edge
Cartesian	2	1	1
Hexahedral	5.4772	2.4534	3
Kershaw	32.0274	5.0012	6

Table 1: Regularity parameter of the meshes and nb of points to approximate the trace-back cells.

the choice of mesh. The solution on the Kershaw mesh is noticeably different, due to the mesh being very distorted; this leads to a skewed approximation of the Darcy velocity, and thus a skewed advection of the fluid.

4 Summary

In previous work, the pressure equation (1a) and the concentration equation (1b) are often treated separately. This work presents a complete scheme for both equations, which is usable on generic meshes as encountered in real-world applications – with the usual caveats on distorted meshes. Our analysis demonstrates the importance of
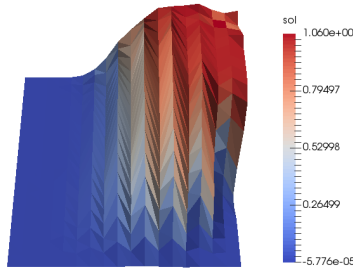
Fig. 10: Kershaw mesh, $t = 3$ years, 6 points per edge, weighted trapezoid rule for source terms.
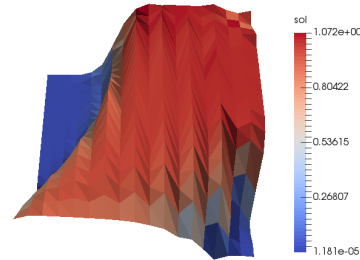

Fig. 11: Kershaw mesh, $t = 10$ years, 6 points per edge, weighted trapezoid rule for source terms.

choosing a proper quadrature rule for integrating the source terms, and of selecting a correct number of approximation points – depending on the regularity of the mesh – to trace the cells. Further research will focus on reducing the grid effects on skewed meshes, and on finding better quadrature rules to deal with larger time steps.

References

1. Arbogast, T., Huang, C.: A fully mass and volume conserving implementation of a characteristic method for transport problems. SIAM Journal on Scientific Computing **28**(6), 2001–2022 (2006)
2. Arbogast, T., Wang, W.H.: Stability, monotonicity, maximum and minimum principles, and implementation of the volume corrected characteristic method. SIAM Journal on Scientific Computing **33**(4), 1549–1573 (2011)
3. Chainais-Hillairet, C., Droniou, J.: Convergence analysis of a mixed finite volume scheme for an elliptic-parabolic system modeling miscible fluid flows in porous media. SIAM J. Numer. Anal. **45**(5), 2228–2258 (electronic) (2007)
4. Droniou, J., Eymard, R., Gallouët, T., Guichard, C., Herbin, R.: The gradient discretisation method (2016). URL https://hal.archives-ouvertes.fr/hal-01382358. Submitted.
5. Droniou, J., Eymard, R., Gallouët, T., Herbin, R.: A unified approach to mimetic finite difference, hybrid finite volume and mixed finite volume methods. Math. Models Methods Appl. Sci. **20**(2), 265–295 (2010)
6. Herbin, R., Hubert, F.: Benchmark on discretization schemes for anisotropic diffusion problems on general grids. In: FVCA V, pp. 659–692. ISTE, London (2008)
7. Kuznetsov, Y., Repin, S.: New mixed finite element method on polygonal and polyhedral meshes. Russian Journal of Numerical Analysis and Mathematical Modelling **18**(3) (2003)
8. Peaceman, D.W., Rachford Jr., H.H.: Numerical calculation of multidimensional miscible displacement. Society of Petroleum Engineers Journal **2**(4), 327–339 (1962)
9. Sweeney, J.: Numerical methods for an oil recovery model (2015). Honours thesis, Monash University.
10. Wang, H., Liang, D., Ewing, R.E., Lyons, S.L., Qin, G.: An approximation to miscible fluid flows in porous media with point sources and sinks by an Eulerian-Lagrangian localized adjoint method and mixed finite element methods. SIAM J. Sci. Comput. **22**(2), 561–581 (electronic) (2000)